Diamond & Related Materials xxx (2010) xxx–xxx

Contents lists available at ScienceDirect

Diamond & Related Materials

journal homepage: www.elsevier.com/locate/diamond

Hydrogenation of nanodiamonds using MPCVD: A new route toward organic functionalization

H.A. Girard [a,b,*], J.C. Arnault [a], S. Perruchas [b], S. Saada [a], T. Gacoin [b], J.-P. Boilot [b], P. Bergonzo [a]

[a] CEA, LIST, Diamond Sensors Laboratory, F-91191 Gif-sur-Yvette, France
[b] Laboratoire de Physique de la Matière Condensée (PMC), CNRS-Ecole Polytechnique, F-91128 Palaiseau Cedex, France

ARTICLE INFO

Article history:
Received 22 December 2009
Received in revised form 10 March 2010
Accepted 23 March 2010
Available online xxxx

Keywords:
Nanodiamonds
Hydrogenation
Surface analysis
Functionalization
Diazonium

ABSTRACT

Nanodiamonds (NDs) emerge as excellent candidates for biological applications but their functionalization is still an issue. By analogy with hydrogenated diamond layers, an efficient and homogeneous covalent functionalization can be achieved on hydrogenated NDs. Here is reported an efficient new approach to hydrogenate NDs by reducing all various oxygenated groups into C–H terminations. The hydrogenation treatment is performed by exposing the nanoparticles to microwave hydrogen plasma in the gas phase. The hydrogenation of the nanoparticles has been carefully characterized by FTIR and XPS analysis revealing strong modification and homogenization of their entire surface. To validate this hydrogen treatment, functionalization of the NDs has been conducted by using diazonium reactions. An efficient grafting was observed for the hydrogenated NDs compared to the as-received ones.

1. Introduction

Recent developments in nanosciences and nanotechnologies have shown that diamond nanoparticles or nanodiamonds (NDs) are of high interest owing to their outstanding mechanical and optical properties associated with their good chemical stability [1–3]. Since the demonstration of their low cytotoxicity [4–6], NDs are considered as promising materials for biological applications [7]. Actually, nanodiamonds are studied for drug delivery applications [8]. NDs exhibit also remarkable luminescence properties with emission of great stability and of high quantum yield which originate from color centers (such as Nitrogen-Vacancy centers), naturally present or induced by ion beam irradiations in the diamond lattice [2,9,10]. Consequently, NDs emerge also as excellent candidates for biolabeling applications [6].

For the development of such applications, functionalization of the NDs is required. The carbon surface of diamond constitutes an excellent support for covalent functionalization. However, as reported in the literature, direct covalent functionalization of NDs appears to be a limiting step, since efficient grafting may be restricted by the complex surface of the raw NDs. Mainly due to oxidizing post-synthesis treatments, NDs are covered by a wide variety of oxygenated functions: hydroxyl, ether, ketones or carboxylic acid groups [10]. This scattered superficial chemistry prevents an efficient and homogenous functionalization due to different reactivity of these various oxygenated groups.

Different experimental pathways have been explored to better control the surface termination of NDs. The first one is the oxidative treatment of NDs with strong acids leading to the formation of COOH groups on the surface which can then react with alcohols or amines derivatives [11–13]. Another approach reported by Krueger et al. [10] consists in reducing all oxygen-containing surface groups to OH functions with borane, then allowing the grafting of a variety of silanes [14] or long alkyl chains [15]. Halogenation of NDs has been also reported such as the thermal fluorination of detonation diamond by Khabashesku and coworkers [16], and the cold-plasma functionalization used by Ray et al. [17]. Fluorinated NDs can then react with nucleophilic reagents in substitution reactions leading to amino or acid terminations [16].

By analogy with diamond films, another promising way to homogenize NDs surface is the hydrogenation. Indeed, by reducing all oxygenated terminations into C–H groups, this treatment ensures a reproducible and versatile surface for further functionalization. Furthermore, hydrogenated terminations confer on diamond films specific electronic properties, allowing particular grafting approaches based on physico-chemical activations. In pioneering works, Hamers and coworkers [18,19] reported on functionalization of hydrogenated diamond surface by photochemical reaction under UV illumination with a long-chain unsaturated amine, being the first step to DNA-modified diamond surface. Based on the same photochemical method, Christiaens and coworkers [20] overcame the problem of insufficient carboxylation by attaching fatty acid chains to the diamond surface and created a universal coupler for amino groups. Still on

* Corresponding author. CEA, LIST, Diamond Sensors Laboratory, F-91191 Gif-sur-Yvette, France.
E-mail address: hugues.girard@polytechnique.edu (H.A. Girard).

0925-9635/$ – see front matter © 2010 Published by Elsevier B.V.
doi:10.1016/j.diamond.2010.03.019

hydrogenated diamond surfaces, Lud et al. [21] presented the grafting of one monolayer of nitrobiphenyl by using the corresponding diazonium salt. Spontaneous reaction of diazonium derivatives on diamond hydrogenated surfaces was also reported by Boukherroub and coworkers in the presence of sodium dodecyl sulfate [22]. In the same way, Shul et al. [23] reported on solvent-free functionalization of hydrogenated surface by aryldiazonium salts in ionic liquids, and suggested that the electron necessary for reduction of diazonium salt are most likely provided by the hydrogenated diamond surface.

By analogy with these works, a large field of functionalization methods is potentially offered to hydrogenated NDs (H-NDs). Indeed, first promising results concerning surface grafting of hydrogenated particles have been recently reported. Yeap et al. [24] has described the functionalization of NDs with aryl organics using Suzuki coupling reaction, starting from partially hydrogenated NDs (presence of hydroxyl groups at the surface) and they showed that diazonium coupling can occur on these NDs. Regarding electronic properties provided by hydrogenated terminations, a detailed study on hydrogenated micrometric diamond powder was conducted by Chakrapani et al. [25]. They demonstrated an electron transfer from the diamond to the surface, deduced from zeta potential measurements, leading to a surface conductivity. It would be interesting to know whether such specific chemical and electronic properties of hydrogenated diamond surfaces can be also obtained on hydrogenated NDs.

To take advantage of the promising properties of H-NDs, the initial treatment conferring the hydrogenated terminations is crucial and has to be carefully optimized. In the literature, only few example of hydrogen treatments performed on NDs deposited onto substrates have been reported, using either atomic hydrogen exposure under ultra-high vacuum (UHV) [26,27] or microwave hydrogen plasma [24,28]. These methods seem to be efficient in terms of surface modification but lead only to a partial hydrogenation of the NDs surface. Moreover, some chemical interactions can take place between NDs and the substrate during the hydrogenation treatment [28]. To the best of our knowledge, there is no reported method providing hydrogenation of the whole NDs surface.

Here, we report on a new approach allowing the full hydrogenation of NDs by exposition to hydrogen Microwave Plasma Chemical Vapor Deposition (MPCVD). NDs are treated in the gas phase allowing the modification of their whole surface by reducing oxygenated terminations into hydrogenated ones. Furthermore, the present method is able to treat a large amount of NDs simultaneously, (hundreds mg), which is a prerequisite to a meaningful surface functionalization. Two kinds of NDs have been studied which are produced either by High Pressure High Temperature (HPHT) or detonation processes. These NDs mainly differ by their size and the graphitic shells surrounding the sp^3 core for detonation NDs [29]. Surface modifications of the NDs induced by the hydrogen plasma exposure have been carefully characterized using X-ray Photoelectron Spectroscopy (XPS) and Fourier Transformed Infra-Red Spectroscopy (FTIR). Finally, to validate the hydrogen treatment, functionalization on these H-NDs has been conducted by using diazonium reactions.

2. Experimental

2.1. Chemicals

High Pressure High Temperature (HPHT) NDs (mean diameter: 50 nm) were purchased from Van Moppes (Syndia® SYP 0-0.05). Detonation diamond NDs (mean diameter of primary particles: 5 nm) were provided by NanoCarbon Research Institute Ltd. Acetonitrile (Riedel-De Haën), pentane (VWR) and 4-nitrophenyldiazonium tetrafluoroborate (Aldrich) were used as received.

2.2. MPCVD hydrogenation

NDs were used as-received. 100 mg of NDs was deposited in a quartz cartridge which was introduced in a quartz tube. This system was introduced into the microwave waveguide cavity (Fig. 1). After a pumping stage, the hydrogen was injected up to 10 mbar. Hydrogen plasma was generated in the quartz tube with a microwave power of 300 W. To limit the temperature of NDs, the quartz cartridge was sequentially removed from the waveguide for few seconds. A rotation of the quartz tube was also applied to mix and homogenize the NDs in the hydrogen plasma. After exposure, H-NDs were collected in dry pentane under hydrogen flux and stored under controlled atmosphere to avoid any spontaneous surface oxidation by air.

2.3. Functionalization

20 mg of as-received or hydrogenated HPHT and detonation nanodiamonds were reacted with 60 mg ($2.5\ 10^{-4}$ mol) of 4-nitrophenyldiazonium tetrafluoroborate in 25 mL of acetonitrile during 12 h. All experiments were conducted under vigorous stirring and under controlled atmosphere. After reaction, NDs were washed by 5 successive centrifugation-redispersion cycles in acetonitrile and then the solid residue was dried under vacuum.

2.4. Characterizations

XPS analyses were performed using an Omicron XPS spectrometer equipped with an Al Kα monochromatized anode ($h\nu = 1486.6$ eV). The binding energy scale was calibrated versus the Au 4f 7/2 peak located at 84.0 eV [30]. The penetration depths are given by the inelastic mean free paths for C1s core levels, close to 3 nm [31]. Curve fitting procedure was performed to extract the components in the C1s spectra, using a fixed Gaussian/Lorentzian ratio of 30%. Peak areas were determined following the Shirley's inelastic background subtraction method. Atomic ratios were calculated from the integrated intensities of core levels after photoionization cross-section corrections. The component ratios C_x/C_{total} correspond to the integrated intensity of each peak C_x over the total area of the C1s spectrum. To avoid air exposure, immediately after hydrogenation a small amount (few mg) of H-NDs (HPHT or detonation) covered with a drop of pentane was deposited on the sample holder and introduced directly in the UHV set-up equipped for surface analysis.

FT-IR spectra were measured in a transmission mode using a Thermo Nicolet 8700 spectrometer. KBr pellets (150 mg) were prepared using 5 mg of as-received, H-NDs (immediately after hydrogenation) or functionalized NDs. Background signal was recorded using a pure KBr pellet. Depending on the experiment, KBr pellets containing or not NDs were dried in a dessicator for one day under primary vacuum.

Powder X-ray diffraction patterns were acquired on a X'Pert Philips diffractometer (40 kV, 40 mA) with CuKα radiation ($\lambda = 0.154056$ nm).

3. Results and discussions

3.1. MPCVD hydrogenation

Hydrogenation of the diamond nanoparticles was performed on as-received HPHT and detonation NDs using MPCVD hydrogen plasma. The experimental set-up is shown on Fig. 1 and described in experimental section. FTIR spectra of as-received and hydrogenated NDs are reported on Fig. 2. For as-received HPHT NDs (Fig. 2a), a broad band is observed at 1775 cm^{-1} characteristic ~~of C O stretching~~ band involved in carboxylic acid groups and anhydride functionalities [32]. This band is less intense for as-received detonation NDs (Fig. 2b), and due to their smaller size the signal is shifted to 1730 cm^{-1} [33]. For

Please cite this article as: H.A. Girard, et al., Diamond Relat. Mater. (2010), doi:10.1016/j.diamond.2010.03.019

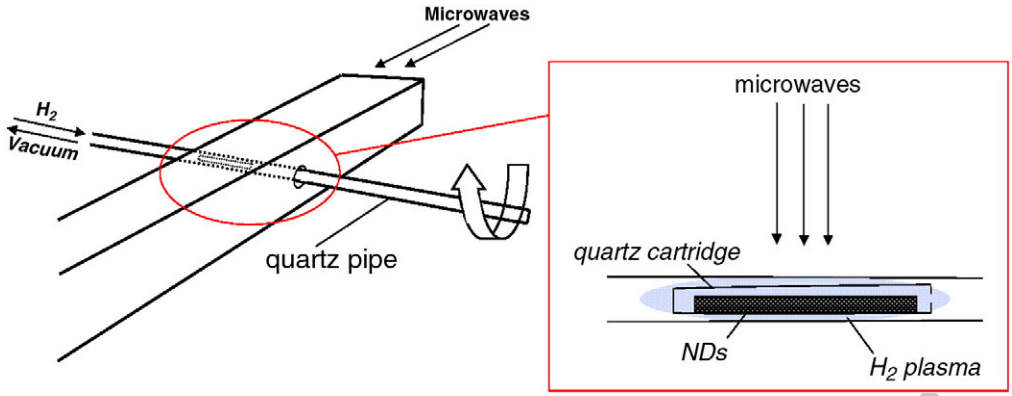

Fig. 1. Experimental set-up used for NDs hydrogenation.

both kinds of NDs, a large band centered at 1050 cm^{-1} indicates the presence of hydroxyl groups. Signals located at 1635 and around 3300 cm^{-1} originate from adsorbed water in the KBr pellet and on NDs [34].

For detonation NDs (Fig. 2b), after a hydrogenation treatment of 10 min, a complete vanishing of the C–OH band at 1050 cm^{-1} is observed, while the C–O bond at 1730 cm^{-1} still remains. After a similar second hydrogenation treatment (10 min), this band completely disappears. Concerning HPHT NDs, after a continuous plasma treatment of 20 min, the strong contribution of the C–O band at 1775 cm^{-1} is totally eliminated as well as the band related to hydroxyl groups at 1050 cm^{-1} (Fig. 2a). For both kinds of NDs, the signals at 1635 and 3300 cm^{-1} are still present on the FTIR spectra after hydrogenation treatment (Fig. 2a–b). Their disappearance after drying the KBr pellet confirms these two bands are related to adsorbed water (Fig. 2). On dried H-NDs, signals located around 2900 cm^{-1} are exalted. These bands have been previously assigned to C–H stretching of the hydrogenated NDs surfaces [35].

XPS analyses were carried out on as-received and H-NDs to investigate surface modifications induced by the hydrogenation treatment. For as-received NDs, XPS spectra exhibit the presence of carbon and oxygen on the NDs. From O1s and C1s core levels areas, atomic concentrations were calculated for as received NDs and led to an oxygen ratio of 18.0 at.% for both kinds of NDs (HPHT and detonation). After hydrogenation, an important decrease of the oxygen peak occurred. An oxygen atomic concentration of 6.6 at.% was estimated for HPHT H-NDs. However, XPS general survey also exhibited the presence of silicon species (2.4 at.%) after the treatment, probably due to a slight degradation of the quartz cartridge. The study of the Si2p core level revealed the presence of SiO_x ($1<x<2$) species and by taking into account the position and the area of the Si2p core level [36], correction of the oxygen atomic concentration was achieved. The corrected value of oxygen linked to NDs was thus estimated to 3 at.% and for both kind of NDs.

Fig. 3 shows the C1s core levels spectra of NDs before and after hydrogenation. For as-received HPHT (Fig. 3a) and detonation NDs (Fig. 3b), a main peak is observed at 286.3 and 286.9 eV respectively which can be assigned to the C–C sp^3 diamond bonds. These two kinds of NDs mainly differ by their oxygen–carbon components located at higher energies between 287 and 292 eV. C1s core level of the as-received HPHT NDs clearly exhibits a component located at 290.5 eV, related to carboxylic groups, and a shoulder between 287 and 289 eV, assigned to hydroxyl and ether functionalities [37]. The broader C1s peak of the as-received detonation NDs (FWHM = 3.0 eV) points out a more important contribution of the components related to hydroxyl and ether groups (between 287 and 289 eV), while the component related to carboxylic groups is weak. These observations are in agreement with the FTIR analysis which shows higher signal for carboxylic groups in the case of HPHT NDs. After hydrogenation, a strong modification of the C1s spectra is observed for both NDs. For HPHT particles (Fig. 3a), a shift of the main peak from 286.3 to 284.9 eV occurs and the full width at half maximum (FWHM) is reduced from 1.8 to 1.3 eV. For detonation NDs, the initial broad C1s core level is also strongly modified with a shift from 286.9 to 285.0 eV associated with a narrower FWHM from 3.0 to 1.5 eV. An important point is that noticeable differences of the C1s core levels exhibited by the as-received HPHT and detonation NDs, especially for high binding energy components, almost disappear after hydrogenation, leading to nearly similar C1s core levels. The narrowness of these peaks also clearly indicates a surface homogenization of the carbon binding

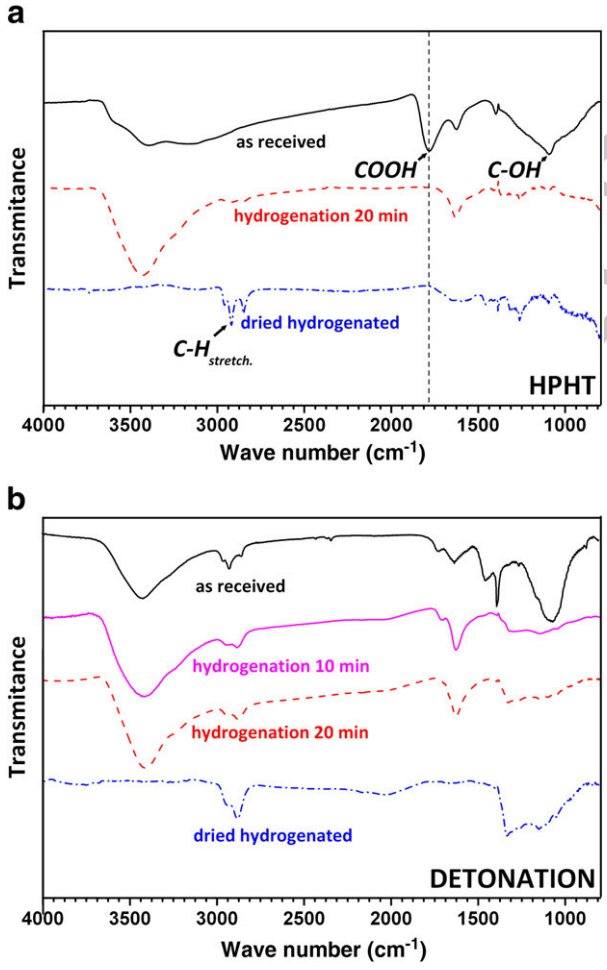

Fig. 2. Transmission FTIR spectra of as-received and hydrogenated (a) HPHT and (b) detonation NDs.

Please cite this article as: H.A. Girard, et al., Diamond Relat. Mater. (2010), doi:10.1016/j.diamond.2010.03.019

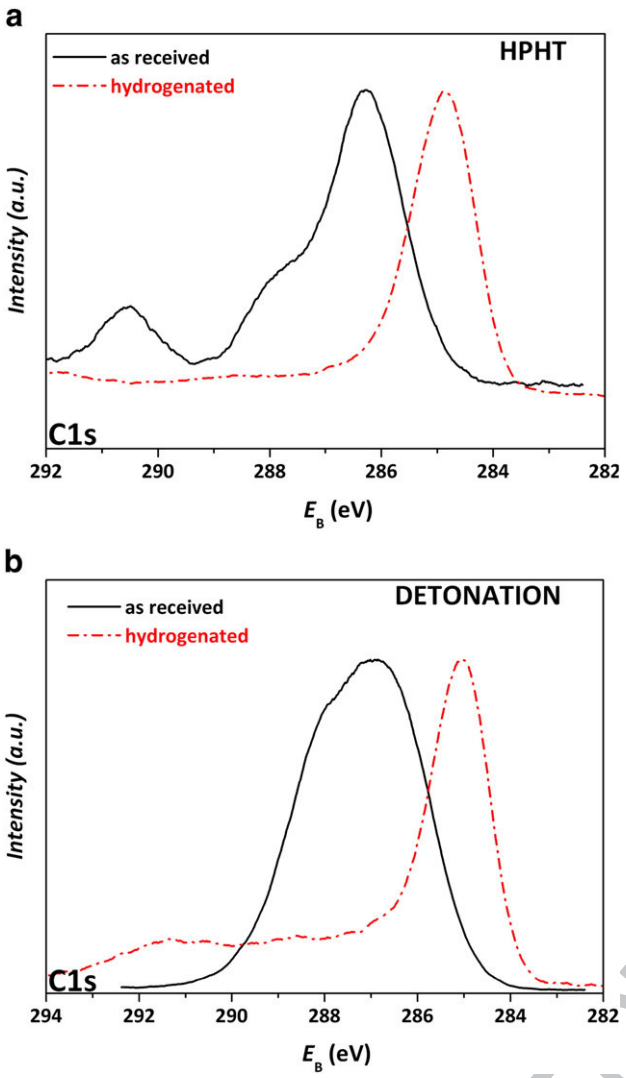

Fig. 3. C1s core levels of as-received and hydrogenated (a) HPHT and (b) detonation NDs.

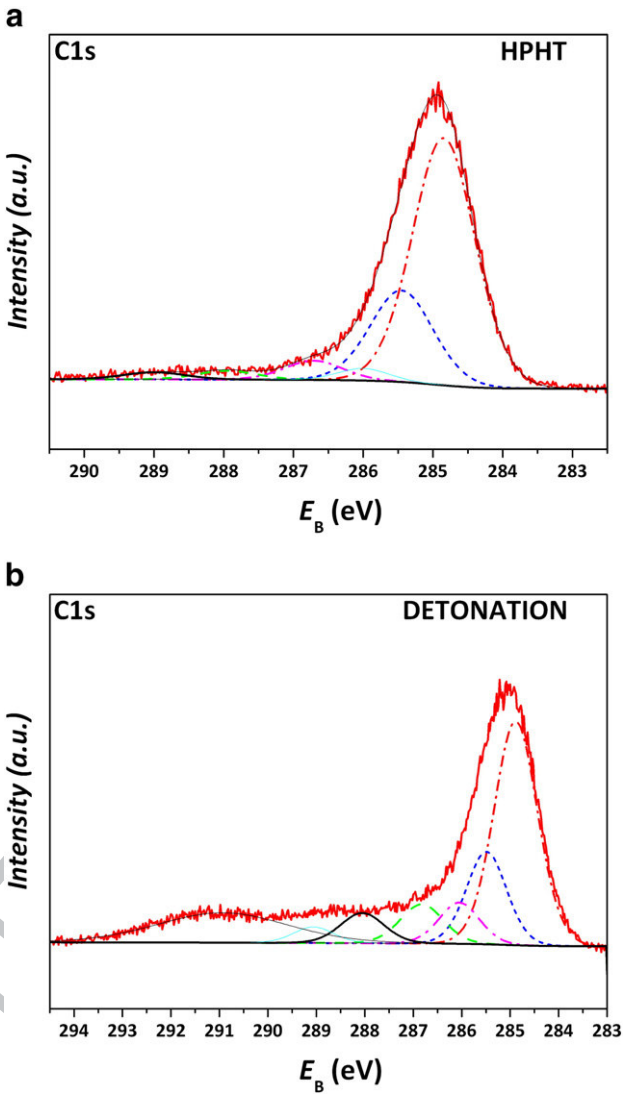

Fig. 4. Deconvolution of C1s core levels of hydrogenated (a) HPHT and (b) detonation NDs.

states with the strong decrease or even the vanishing of some high binding energy components related to carbon–oxygen bonds.

To deeply analyze the H-NDs spectra, deconvolution of the C1s core level spectra was performed (Fig. 4). For the HPHT H-NDs (Fig. 4a), the two main components located at 284.8 and 285.4 eV can be assigned to C–C sp^3 and CH_x bonds, respectively [38]. No C–C sp^2 contribution has been detected which is usually located at lower binding energy compared to C–C sp^3 [37]. At higher binding energies, four weaker contributions located at 286, 286.7, 287.9 and 289 eV could be assigned to oxygenated terminations. Similarly, deconvolution of the C1s core level of detonation H-NDs (Fig. 4b) revealed two main peaks related to C–C sp^3 and CH_x bonds and also contributions at higher binding energies. A supplementary component located at very high binding energies (290.9 eV) is also observed, but without chemical significance. However, when XPS analyses were performed on different areas of the samples, the intensity of these high energy contributions (between 286 and 291 eV) fluctuate while those of the main components (C–C sp^3 and CH_x) do not change. Moreover, the atomic oxygen content calculated from O1s core level remained close to 3 at.% whatever the proportion of high energy components in the C1s core level . This phenomenon suggests that the components located at high binding energies are not related to C/O chemical bonds on the NDs, but to an experimental artefact, such as charging effects. Indeed, compared to the as-received NDs, hydrogenated NDs are probably highly insulating due to the surface cleaning by the hydrogen plasma. Furthermore their deposition on the sample holder led to the formation of aggregates due to their hydrophobic character. Consequently, charging effect under photon illumination is strongly conceivable on our samples. This charge build-up leads to the deformation of the core levels between 286 and 291 eV, with some difference between HPHT and Detonation NDs probably due to a size effect [26] and an inhomogeneous deposition on the sample holder.

To summarize, from FTIR analyses, oxygenated terminations initially present on NDs surface were removed by hydrogenation plasma, including carboxylic and hydroxyl groups. This qualitative analysis points out the hydrogenation efficiency in term of surface homogenization. Additionally, as transmission FTIR probes the whole sample, we have a clear indication that the entire NDs surface has been treated by the MPCVD plasma. Yeap et al. mentioned that hydroxyl groups remain after hydrogenation [24] (from FTIR analysis), but the comparison is difficult because no details about their experimental conditions are given. In our case, XPS analyses confirmed the hydrogenation with quantitative data. The oxygen atomic concentration drops from 18 at.% to 3 at.%. Despite of charging effect, a severe removal of the C/O components is observed at the C1s core levels. The presence of this small oxygen percentage on the surface has to be discussed. Indeed, the transfer of the H-NDs from the

Please cite this article as: H.A. Girard, et al., Diamond Relat. Mater. (2010), doi:10.1016/j.diamond.2010.03.019

hydrogenation set-up to the XPS spectrometer was fast and carefully controlled but a slight exposition to air cannot be avoided leading to a partial re-oxidation of the particles. Additionally, as shown by XPS analysis, a weak degradation of the quartz cartridge occurred during exposure to the microwave plasma which may introduce oxygen species in the gas phase during the treatment. In addition to the clear removal of the main oxygenated terminations on H-NDs evidenced by FTIR and XPS, we also have signatures of the hydrogenated terminations. After water desorption, FTIR spectra of H-NDs exhibited typically C–H stretching bands of a hydrogenated diamond surface (Fig. 2a). Moreover, XPS analyses showed an important displacement of C1s core levels to lower binding energies after treatment, which is in agreement with hydrogenated diamond surfaces [39,40]. For both kinds of H-NDs, C–C sp^3 components were measured at 284.8 eV and this later value is in accordance with binding energies typically measured on undoped hydrogenated diamond thin films [41]. The position and narrowness of this peak is undoubtedly a signature of an efficient surface hydrogenation of both kinds of NDs.

Powder X-ray diffraction analyses were performed to study the effect of the hydrogenation on the crystalline structure of the particles. Diffraction patterns are shown in Fig. 5 for HPHT and detonation NDs. All spectra show the characteristic (111) peak of the diamond structure at $2\theta = 44°$. For both HPHT and detonation NDs, no modification of this peak is observed after hydrogenation. Average crystallites sizes were calculated from FWHM using Scherrer formula [42] and give a diameter of 16 nm for HPHT NDs and 4 nm for detonation ones. Thus, the size of the diamond core of the NDs is not modified upon hydrogenation, thus confirming that this treatment is restricted to the NDs surface.

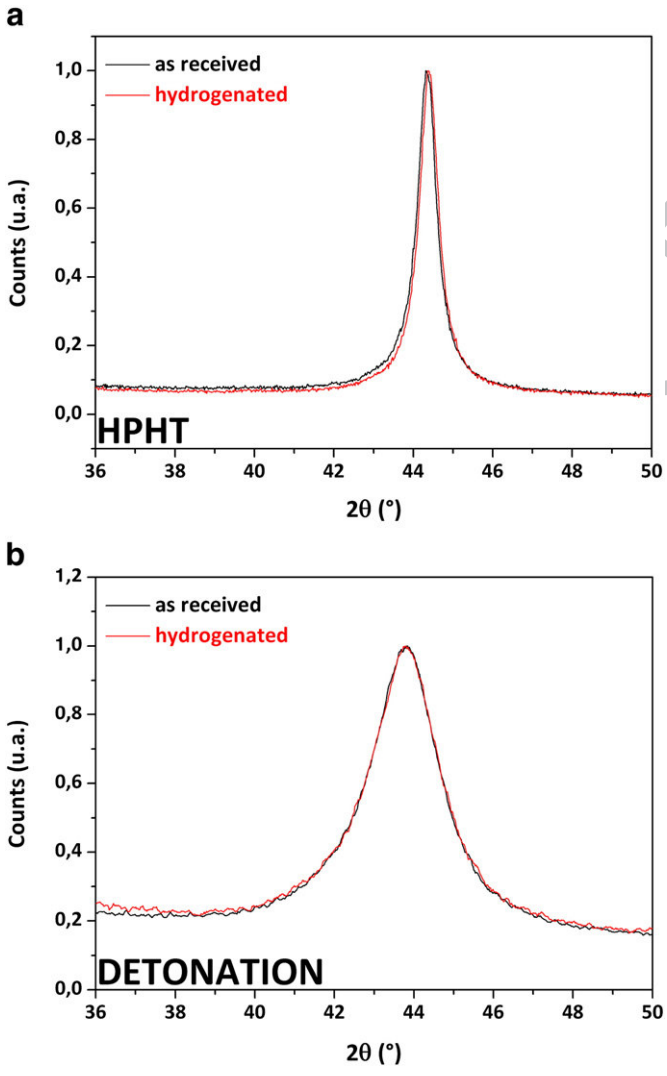

Fig. 5. X-ray diffraction patterns of (a) HPHT and (b) detonation NDs before and after hydrogenation.

3.2. Functionalization

In order to validate the hydrogenation of the NDs, we have investigated their functionalization. As reported for diamond layers, diazonium coupling is known to be very efficient on hydrogenated diamond [21–23]. Therefore, this reaction has been conducted on both as-received and hydrogenated NDs for comparison. Both NDs were then reacted in exactly the same conditions with the nitrobenzene diazonium salt as reported on Fig. 6. Fig. 7a and b show the corresponding FTIR spectra after reaction on HPHT and detonation NDs as well as the one of the nitrobenzene diazonium salt reactant for comparison.

FTIR spectrum of the nitrobenzene diazonium shows one stretching vibration band related to the N≡N function at 2280 cm^{-1}, as well as two intense bands corresponding to the symmetric and antisymmetric ONO stretching vibrations at 1344 and 1520 cm^{-1} respectively. After reaction of the HPHT H-NDs with the diazonium salt, the two bands related to the NO_2 group are clearly present at 1344 and 1520 cm^{-1}, whereas no signal corresponding to the N≡N function is observed. On the FTIR spectra of as-received NDs, no signature of the ONO stretching vibrations was noticeable, while the C=O stretching band at 1775 cm^{-1} is still clearly observable. On detonation NDs, signatures of the NO_2 groups are also only observable on previously hydrogenated NDs. XPS analyses performed on HPHT samples revealed a nitrogen atomic concentration of 3.3 at.% for the functionalized H-NDs (Fig. 7b), with an unambiguous component at 406 eV related to NO_2 groups on the N1s core level [43] (insert Fig. 7b). Note that no signature of the BF_4^- counter-ion was noticed on the XPS spectra confirming the reaction of the diazonium salt. For the as-received NDs, no component around 406 eV was detected and the nitrogen atomic concentration was evaluated at 0.4 at.%.

These results evidenced that the spontaneous coupling of the diazonium derivative occurs only on the H-NDs. This reaction is confirmed by the FTIR and XPS signatures of the NO_2 groups, but also by the lack of N≡N signal on the FTIR spectrum pointing out the grafting of the nitrobenzene group through a covalent bond. From the 3.3 at.% of nitrogen of XPS analysis, we can estimate the surface density of nitrophenyl groups grafted on the NDs between 0.5 and 1 function/nm^2. This value lies in the same range of density reported for functionalized diamond films in similar conditions (3 molecule/nm^2) corresponding to a densely packed monolayer of nitrophenyl groups [21]. It is important to note that this reaction was conducted on H-NDs only under a vigorous stirring, whereas the grafting of diazonium salts on as-received NDs assisted by ultrasonication has been reported [44]. In the latter case, a lower rate of grafting has been obtained with 0.3 at.% of nitrogen for XPS analysis. Our results are consistent with this study and show that spontaneous diazonium coupling is only efficient on hydrogenated NDs suggesting an activated grafting by the hydrogenated surface, as it is reported for hydrogenated diamond thin films. The hydrogenation efficiency of the NDs surface is thus confirmed by this selective functionalization.

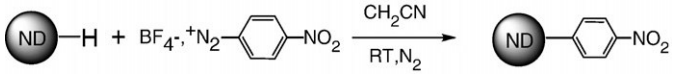

Fig. 6. Scheme of the reaction conducted to functionalize H-NDs and as-received NDs.

Please cite this article as: H.A. Girard, et al., Diamond Relat. Mater. (2010), doi:10.1016/j.diamond.2010.03.019

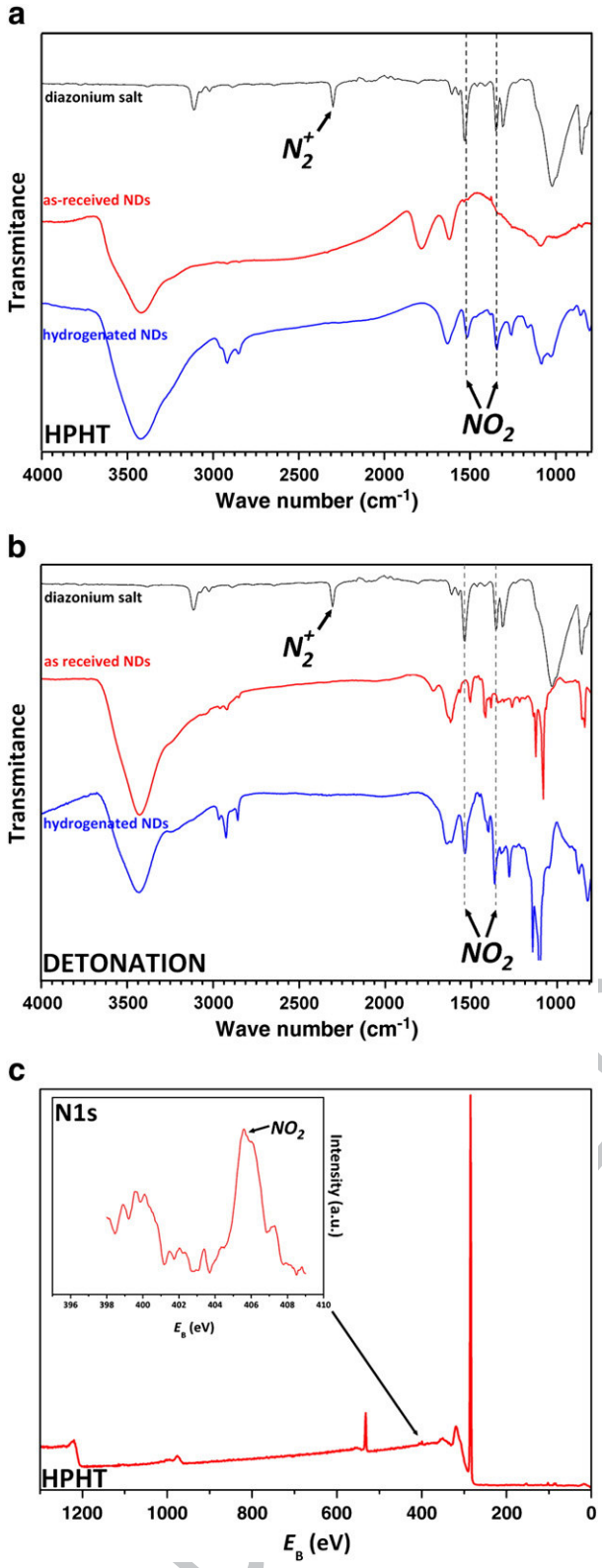

Fig. 7. FTIR spectra of reacted as-received and hydrogenated (a) HPHT and (b) detonation NDs and of the nitrobenzene diazonium salt (c) XPS survey of functionalized hydrogenated HPHT NDs and in insert the N1s core level.

4. Conclusion

This study reports a new approach for NDs hydrogenation conferring hydrogenated terminations to their whole surface. This efficient surface treatment is performed by exposing NDs located in the gas phase to hydrogen microwave plasma. Hydrogenation modified the surface of the NDs without altering their crystalline sp^3 diamond core. This treatment allows the hydrogenation of large amount of NDs of about hundred milligrams. Two kinds of NDs (HPHT and detonation) have been successfully hydrogenated giving rise to similar homogeneous hydrogenated surfaces. FTIR and XPS analyses well evidenced the removal of the oxygenated groups initially present on NDs surface as well as typical signatures of hydrogenated terminations. Hydrogenated NDs exhibit very close spectroscopic characteristics compared to hydrogenated diamond layers especially for the XPS C1s core level. Functionalization of NDs by diazonium coupling has been realised showing spontaneous coupling only on H-NDs compared to as-received NDs. This efficient grafting through covalent bonds validates the hydrogenation treatment.

As already mentioned in the Introduction ~~section~~, hydrogen terminations are known to confer specific physico-chemical properties to diamond surfaces, allowing specific derivatization routes. The latters can be thus applied to hydrogenated nanoparticles opening the route to new strategies for the functionalization of NDs. This is currently under investigation in our laboratories. Moreover, the electronic properties of H-NDs will be studied and compared to hydrogenated films.

Acknowledgments

The authors thank the CNRS for financial support. H.A. Girard thanks the NADIA project (ANR-PNANO 07-045) for the postdoctoral fellowship.

References

[1] A. Krueger, Adv. Mater. 20 (2008) 2445.
[2] M. Baidakova, A. Vul, J. Phys. D: Appl. Phys. 40 (2007) 6300.
[3] V. Jacques, E. Wu, F. Grosshans, F. Treussart, P. Grangier, A. Aspect, J.-F. Roch, Science 315 (2007) 966.
[4] A.M. Schrand, H. Huang, C. Carlson, J.J. Schlager, E. Osawa, S.M. Hussain, L. Dai, J. Phys. Chem. B 111 (2007) 2.
[5] J.I. Chao, et al., Biophys. J. 93 (2007) 2199.
[6] K.K. Liu, Nanotechnology 19 (2008) 205102.
[7] A.M. Schrand, S.A. Ciftan Hens, O.A. Shenderova, Crit. Rev. Solid State Mater. Sci. 34 (2009) 18.
[8] H.J. Huang, E. Pierstorff, E. Osawa, D. Ho, ACS Nano 2 (2008) 203.
[9] A. Gruber, A. Dräbenstedt, C. Tietz, L. Fleury, J. Wrachtrup, C. Von Borczyskowsky, Science 276 (1997) 2012.
[10] A. Kruger, Y. Liang, G. Jarre, J. Stegk, J. Mater. Chem. 16 (2006) 2322.
[11] K. Ushizawa, Y. Sato, T. Mitsumori, T. Machinami, T. Ueda, T. Ando, Chem. Phys. Lett. 351 (2002) 105.
[12] V.M. Mochalin, Y. Gogotsi, J. Am. Chem. Soc. 131 (13) (2009) 4594.
[13] L.-C.L. Huang, H.-C. Chang, Langmuir 20 (2004) 5879.
[14] A. Krueger, J. Stegk, Y. Liang, L. Lu, G. Jarre, Langmuir 24 (2008) 4200.
[15] A. Krueger, T. Boedeker, Diamond Relat. Mater. 17 (2008) 1367.
[16] Y. Liu, Z. Gu, J. Margrave, V. Khabashesku, Chem. Mater. 16 (2004) 3924.
[17] M. Ray, O. Shenderova, W. Hook, A. Martin, V. Grishko, T. Tyler, G. Cunningham, G. McGuire, Diamond Relat. Mater. 15 (2006) 1809.
[18] W.S. Yang, O. Auciello, J.E. Butler, W. Cai, J.A. Carlisle, J. Gerbi, D.M. Gruen, T. Knickerbocker, T.L. Lasseter, J.N. Russell, L.M. Smith, R.J. Hamers, Nat. Mater. 1 (2002) 253.
[19] T. Strother, T. Knickerbocker, J. Russell, J. Butler, L. Smith, R. Hamers, Langmuir 18 (2002) 968.
[20] P. Christiaens, V. Vermeeren, S. Wenmackers, M. Daenen, K. Haenen, M. Nesládek, M. vandeVen, M. Ameloot, L. Michiels, P. Wagner, Biosens. Bioelectron. 22 (2006) 170.
[21] S. Lud, M. Steenackers, R. Jordan, P. Bruno, D. Gruen, P. Feulner, J. Garrido, M. Stutzmann, J. Am. Chem. Soc. 128 (2006) 16884.
[22] S. Szunerits, R. Boukherroub, J. Solid State Electrochem. 12 (2008) 1205.
[23] G. Shul, P. Actis, B. Marcus, M. Opallo, R. Boukherroub, S. Szunerits, Diamond Relat. Mater. 17 (2008) 1394.
[24] W.S. Yeap, S. Chen, K.P. Loh, Langmuir 25 (2009) 185.
[25] V. Chakrapani, J.C. Angus, A.B. Anderson, S.D. Wolter, B.R. Stoner, G.U. Sumanasekera, Science 318 (2007) 1424.
[26] M. Yeganeh, P.R. Coxon, A.C. Brieva, V.R. Dhanak, L. Siller, Y.V. Butenko, Phys. Rev. B 75 (2007) 155404.
[27] C.L. Cheng, C.F. Chen, W.C. Shaio, D.S. Tsai, K.H. Chen, Diamond Relat. Mater. 14 (2005) 1455.
[28] J.C. Arnault, S. Saada, M. Nesladek, O. Williams, K. Haenen, P. Bergonzo, E. Osawa, Diamond Relat. Mater. 17 (2008) 1143.
[29] L.A. Bursill, J.L. Peng, S. Prawer, Philos. Mag. 76 (1997) 769.

[30] M.P. Seah, Surf. Interface Anal. 14 (1989) 488.
[31] S. Tanuma, C.J. Powell, D.R. Penn, Surf. Interface Anal. 11 (1988) 577.
[32] P. Chung, E. Perevedentseva, J. Tu, C. Chang, C. Cheng, Diamond Relat. Mater. 15 (2006) 622.
[33] J. Tu, E. Perevedentseva, P. Chung, C. Cheng, J. Chem. Phys. 125 (2006) 174713.
[34] O. Shenderova, I. Petrov, J. Walsh, V. Grichko, T. Tyler, G. Cunningham, Diamond Relat. Mater. 15 (2006) 1799.
[35] C. Cheng, C. Chen, W. Shaio, D. Tsai, K. Chen, Diamond Relat. Mater. 14 (2005) 1455.
[36] A. Strass, P. Bieringer, W. Hansch, V. Fuenzalida, A. Alvarez, J. Luna, I. Martil, F.L. Martinez, I. Eisele, Thin Solid Films 349 (1999) 135.
[37] S. Ferro, M. Dal Colle, A. De Battisti, Carbon 43 (2005) 1191.
[38] L. Ley, R. Graupner, J.B. Cui, J. Ristein, Carbon 37 (1999) 793.
[39] R. Graupner, F. Maier, J. Ristein, L. Ley, C. Jung, Phys. Rev. B 57 (1998) 12397.
[40] K. Bobrov, G. Comtet, G. Dujardin, L. Hellner, Phys. Rev. B 63 (2001) 165421.
[41] D. Ballutaud, N. Simon, H. Girard, E. Rzepka, B. Bouchet-Fabre, Diamond Relat. Mater. 15 (2006) 716.
[42] R. Jenkins, R.L. Snyder, X-ray Powder Diffractometry, Wiley-Interscience, New York, 1996, p. 89.
[43] B.J. Lindberg, K. Hamrin, G. Johansson, U. Gelius, A. Fahlmann, C. Nordling, K. Siegbahn, Phys. Scr. 1 (1970) 286.
[44] C. Mangeney, Z. Qin, S.A. Dahoumane, A. Adenier, F. Herbst, J.P. Boudou, J. Pinson, M.M. Chehimi, Diamond Relat. Mater. 17 (2008) 1881.

Please cite this article as: H.A. Girard, et al., Diamond Relat. Mater. (2010), doi:10.1016/j.diamond.2010.03.019